COMMISSIONS G1 AND G4 OF THE IAU
INFORMATION BULLETIN ON VARIABLE STARS
Volume 63 Number 6203 DOI: 10.22444/IBVS.6203

Konkoly Observatory
Budapest
06 April 2017

HU ISSN 0374 – 0676

V2197 Cyg – A SEMI-DETACHED ECLIPSING BINARY?

NELSON, ROBERT H.[1,2]; ROBB, RUSSELL M.[2,3]

[1] 1393 Garvin Street, Prince George, BC, Canada, V2M 3Z1, email: bob.nelson@shaw.ca

[2] Guest investigator, Dominion Astrophysical Observatory, Herzberg Institute of Astrophysics, National Research Council of Canada

[3] Department of Physics and Astronomy, University of Victoria, Victoria, B.C., Canada, V8P 2W7

The variability of V2197 Cyg (NSVS 5761314, TYC 3167-1279-1), amongst many others, was discovered photographically by Margoni & Stagni (1984, hereafter M&S) who gave coordinates, magnitude ranges in B and V, finder charts for all 99 stars, elements (epoch, period), and preliminary light curves for about half the stars (but not for V2176 Cyg, their #58). Andronov et al. (1993) performed U, B, V, R, and I photometry of this and three other M&S stars; they went on in Andronov et al. (1994) to identify the system as an eclipsing variable, also giving the elements (including period = 0.46771 d) and eclipse duration. Skiff (1997) identified the M&S variables with those in the IRAS and GSC catalogues. Hoffman et al. (2008) provided an updated period, quoted 2MASS colours, and classified the system as β Lyrae. Since then, there have been a number of eclipse timings but no light curve analysis.

Light curve and radial velocity data have been acquired, but before any analysis could be performed, the first task was to examine the period variation. An eclipse timing difference (O–C) plot using all available data and the elements of Kreiner (2004) is reproduced in Fig. 1.

It will be seen that, even though all data are electronic (PE or CCD), there is a fair amount of scatter–larger than most of the error ranges. Clearly there must be unexplained physical reason for this discrepancy; future accurate data are required to sort out true relationship. In the meantime, the line of best fit must suffice. In view of the fact that all data were taken between cycles 7000 and 9000 (approximately), any errors due to uncertainties in the period are likely to be small.

A slightly different set of elements, specified in equation (1) was used in all phasing.

$$\mathrm{JD\,(Hel)\,Min\,I} = 2457514.9187(5) + 0.4657489(1)E \tag{1}$$

In August of 2012, the lead author took 82 frames in V, 79 in R_C (Cousins) and 77 in the I_C (Cousins) band at his private observatory in Prince George, BC, Canada. The telescope was a 33 cm f/4.5 Newtonian on a Paramount ME mount; the camera was an SBIG ST-10XME. Standard reductions were then applied. The variable, comparison and check stars are listed in Table 1. The coordinates and magnitudes for all three stars are

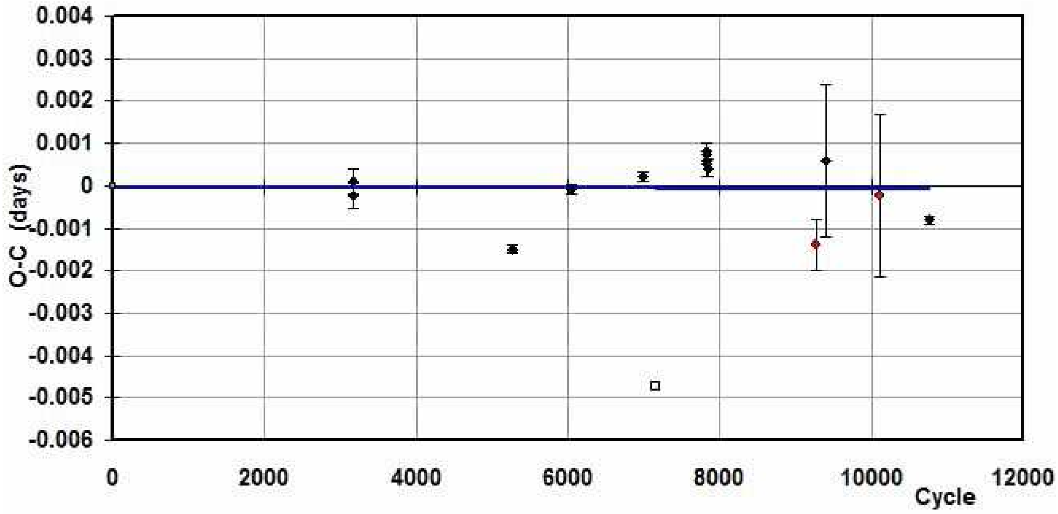

Figure 1. V2197 Cyg – eclipse timing (O–C) diagram. Legend: filled circles – photoelectric; black diamonds – CCD. The open square represents a rejected reading.

Table 1: Details of variable, comparison and check stars.

Object	GSC	RA (J2000)	Dec (J2000)	V (mag)	$B-V$ (mag)
Variable	3167-1279	$20^h50^m16\overset{s}{.}321$	$37°56'45\overset{''}{.}29$	12.04(17)	+0.17(22)
Comparison	3167-0649	$20^h50^m32\overset{s}{.}961$	$37°57'48\overset{''}{.}77$	10.47(4)	+0.30(6)
Check	3167-1451	$20^h50^m13\overset{s}{.}62$	$37°55'54\overset{''}{.}3$	11.66(na)	1.28(na)

from the Tycho Catalogue (Hog et al. 2000) and the 2MASS catalogue, (Cutri et al. 2003), except for the magnitudes of the check star, for which there was no reference in SIMBAD.

In September of 2011, 2013, and 2014, the lead author then took a total of 7 medium resolution (R $\sim$ 10000 on average) spectra of V2197 Cyg at the Dominion Astrophysical Observatory (DAO) in Victoria, British Columbia, Canada using the Cassegrain spectrograph attached to the 1.85 m Plaskett Telescope. He used the 21181 grating with 1800 lines/mm, blazed at 5000 Å giving a reciprocal linear dispersion of 10 Å/mm in the first order. The wavelengths ranged from 5000 to 5260 Å, approximately. A log of observations is given in Table 2. (The last value for V2 listed in the table, –270.7 km/s, was not used in the modelling on the grounds that it was deviant by more than 3σ from the curve of best fit; however, it is plotted in Fig. 6 for reference.)

Frame reduction was performed by software 'RaVeRe' (Nelson 2009). See Nelson et al. (2014) for further details.

Radial velocities were determined using the Rucinski broadening functions (Rucinski 2004; Nelson 2010b; Nelson et al. 2014). An Excel worksheet with built-in macros (written by him) was used to do the necessary radial velocity conversions to geocentric and back to heliocentric values (Nelson 2010a). The resulting RV determinations are also presented in Table 2. For all the data, the results were corrected typically 5 % up to allow for the small phase smearing. Correction was achieved by dividing the RVs by the factor $f = (\sin X)/X$; where$X = 2\pi\, t/P$, and where t denotes exposure time and P denotes the orbital period. For spherical stars, this correction is exact; in other cases, it can be shown to be close enough for any deviation to fall below observational errors. The mean

Table 2: Log of DAO observations.

DAO Image #	Mid Time (HJD−2400000)	Exposure (sec)	Phase at Mid-exp	V_1 (km/s)	V_2 (km/s)
7849	55808.9875	3561	0.229	–148.0	+159.8
8141	55820.6522	3600	0.274	–142.0	+172.0
8153	55820.9065	3600	0.820	+89.4	–217.9
8217	55825.8105	2876	0.350	–134.4	+140.5
9629	56544.6973	3600	0.857	+77.8	–205.6
9638	56544.8504	3600	0.186	–131.0	+174.0
24359	56906.9975	3600	0.745	+97.9	–270.7

rms errors for RV_1 and RV_2 were 9.1 and 14.0 km/s, respectively, and the overall rms deviation from the (sinusoidal) curves of best fit was 12.3 km/s. The best fit yielded the values $K_1 = 123.0(8)$ km/s, $K_2 = 214.3(1.1)$ km/s and $V_\gamma = -30.8(6)$ km/s, and thus a mass ratio $q_{sp} = K_1/K_2 = M_2/M_1 = 0.574(5)$.

One of the authors (R.M.R.) obtained a spectrum of V2197 Cyg at the Dominion Astrophysical Observatory (DAO) with the 1.85 m telescope and the 2131 Cassegrain spectrograph, operating at a reciprocal dispersion of about 60 Å/mm and 0.9 Å/px. The start time of the exposure was 2013 June 22 at UT+09:25:33 and lasted 666 s (JD 2456465.8927), corresponding to phase 0.66. The strength of the G-Band and Hydrogen lines indicate F3(±1)V. A comparison spectrum of 48 Boo (F3V) observed with the same configuration is plotted for comparison in Fig. 2, where the spectra have been scaled and offset an arbitrary amount. The spectrum of V2197 Cyg has been smoothed with a 3 point running average. The lines are (left to right) Ca II K-line, Ca II H-line blended with Hϵ, Hδ, and Hγ.

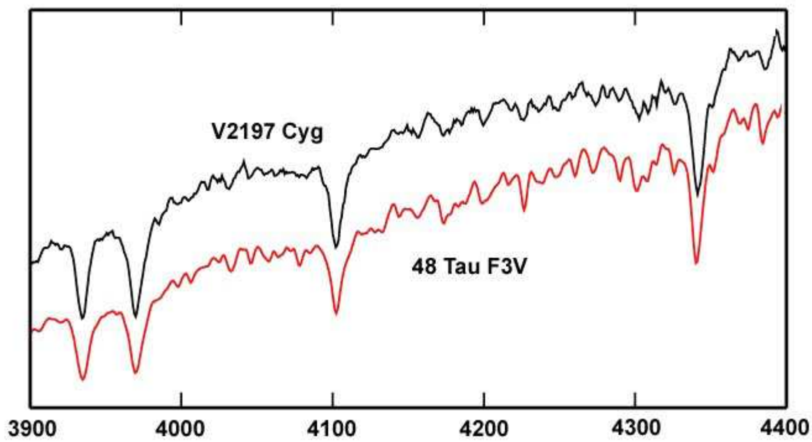

Figure 2. Classification spectra.

Next, the lead author (R.H.N.) used the 2003 version of the Wilson-Devinney (WD) light curve and radial velocity analysis program with Kurucz atmospheres (Wilson and Devinney 1971; Wilson 1990; Kallrath et al. 1998) as implemented in the Windows front-end software WDwint (Nelson 2009) to analyze the data. Using the spectral type of F3V,

Table 3: Limb darkening values from Van Hamme (1993) for $T_1 = 6820$ K and $T_2 = 5037$ K.

Band	x_1	x_2	y_1	y_2
Bol	0.639	0.643	0.249	0.160
V	0.696	0.797	0.284	0.107
R_C	0.622	0.735	0.291	0.165
I_C	0.537	0.647	0.280	0.183

the tables of Cox (2000), and those of Flower (1996) gave a temperature $T_1 = 6820 \pm 200$ K and $\log g_1 = 4.328 \pm 0.012$. (The quoted errors refer to one and one half spectral subclasses.) An interpolation program by Terrell (1994, available from Nelson 2009) gave the Van Hamme (1993) limb darkening values; and finally, a logarithmic (LD = 2) law for the limb darkening coefficients was selected, appropriate for temperatures < 8500 K (ibid.). The limb darkening coefficients are listed below in Table 3. (The values for the second star are based on the later-determined temperature of 5037 K and assumed spectral type of K2.) Convective envelopes for both stars were used, appropriate for cool stars (hence values gravity exponent $g = 0.32$ and albedo $A = 0.500$ were used for each).

From the shape of the light curve, it was clear that the system was in near contact but the difference in the depths of the two minima indicate that the stars are not in thermal contact. Various modes were tried: mode 3 (contact), mode 2 (detached), mode 5 (Algol) and, finally mode 6 (double contact). Convergence was obtained by the method of multiple subsets: (a, V_γ, L_1), (T_2, q), (i, T_2) and (T_2, Ω_1). The net result was residuals (or, more correctly, sums of residuals squared) that were nearly identical, making it difficult to choose between the scenarios. A useful procedure was to proceed with mode 6 (because the potentials were fixed from the mass ratio, thereby reducing the number of free parameters), find the optimum using differential corrections, then switch to another mode, making slight adjustments in potentials Ω_1 and Ω_2 as necessary to satisfy the conditions for that mode, then proceeding with differential corrections once again. This led to the best minimum. Mode 3 failed because differential corrections wanted increases in potential Ω_1 that would force star 1 inside the Roche lobe (i.e., $\Omega_1 > \Omega_i$ where the latter is the inner critical potential), and in any case, the unequal depths of minima precluded this mode. Mode 2 (detached) also failed for the same reason, except that this time, differential corrections wanted potential $\Omega_2 > \Omega_i$, that is for the secondary to be at or inside the Roche lobe. Therefore only mode 5 (semi-detached) and mode 6 (double contact) remained.

In the first set of iterations when the fit was near, the sigmas for each dataset were adjusted, based on the output of WD (viz. computed from the sum of residuals for each dataset plus number of points). The same values were then used throughout in order that results from the different iterations could be compared.

It would seem that mode 5 (semi-detached) gave the best solution, but only by a very small margin. Also, in view of the errors in the data, it seems clear that another data set might well favour a different mode. Therefore one cannot in confidence differentiate between the two modes. On the other hand, all produce virtually identical fundamental parameters—certainly well within the estimated errors.

Detailed reflections were tried, with $n_{ref} = 2$, but there was little—if any—difference in the fit from the simple treatment. There are certain uncertainties in the process (see Csizmadia et al. 2013; Kurucz 2002). On the other hand, the solution is very weakly dependent on the exact values used.

Solutions were tested for third light; suggested corrections were smaller than estimated

Table 4: Wilson-Devinney parameters.

WD Quantity	Mode 5	Mode 6	error	unit
Temperature T_1	6820	6820	[fixed]	K
Temperature T_2	5037	5037	12	K
$q = m_2/m_1$	0.595	0.595	0.018	—
Potential Ω_1	3.0551	3.0542	0.063	—
Potential Ω_2	3.0542	3.0542	—	
Inclination, i	80.20	80.20	0.07	deg
Semi-maj. axis a	3.182	3.182	0.056	$R_\odot$
Syst. velocity, V_γ	–25.2	–25.2	0.6	km/s
Phase shift	0.0011	0.0011	0.0001	—
$L_1/(L_1 + L_2)\,(V)$	0.8743	0.8744	0.0002	—
$L_1/(L_1 + L_2)\,(R_C)$	0.8455	0.8456	0.0002	—
$L_1/(L_1 + L_2)\,(I_C)$	0.8195	0.8197	0.0002	—
r_1 (pole)	0.3996	0.3997	0.0023	orb. rad.
r_1 (point)	0.5253	0.5532	0.1387	orb. rad
r_1 (side)	0.4229	0.4231	0.0032	orb. rad.
r_1 (back)	0.4517	0.4519	0.0052	orb. rad.
r_2 (pole)	0.3136	0.3136	0.0022	orb. rad.
r_2 (point)	0.4468	0.4468	0.0085	orb. rad
r_2 (side)	0.3277	0.3277	0.0024	orb. rad.
r_2 (back)	0.3599	0.3599	0.0023	orb. rad.
$\sum \omega_{res}^2$	0.02513	0.02519	—	—

errors. Therefore third light was eliminated. In spite of the fact that spots might be expected on one or other stars, no attempt was made to include them, as there was no need. It seems likely that any indication of a spot occurring on the secondary would be overwhelmed by the light of the primary.

The two acceptable solutions are presented in Table 4. For the most part, the error estimates are the formal errors provided by the WD routines and are known to be low; the actual errors may be several times the quoted ones. However, it is a common practice to quote these estimates, and we do so now. Also, estimating the uncertainties in temperatures T_1 and T_2 is somewhat problematic. A common practice is to quote the temperature difference over—say—1.5 spectral sub-classes (assuming that the classification is good to one spectral sub-class). In addition, various different calibrations have been made (Cox 2000, page 388–390 and references therein; and Flower 1996), and the variations between the various calibrations can be significant. Here a spectral type (for star 1) was determined to be F3($\pm$1) sub-classes. Then the uncertainty over one and one half spectral sub-classes gives an uncertainty of $\pm$200 K to the absolute temperatures of each. The modelling error in temperature T_2, relative to T_1, is indicated by the WD output to be much smaller, around 12 K.

The light curve data and the fitted curves are plotted in Figures 3–5. The residuals (in the sense observed-calculated) are also plotted, shifted upwards by 0.40 units.

The radial velocities and the fit are plotted in Fig. 6. A three-dimensional representation from Binary Maker 3 (Bradstreet, 1993) is depicted in Fig. 7.

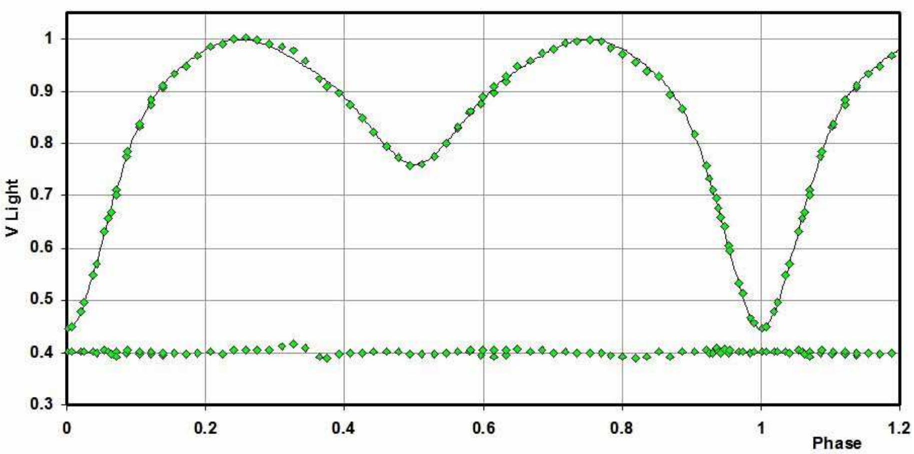

Figure 3. V light curves for V2197 Cyg – data, WD fit, and residuals.

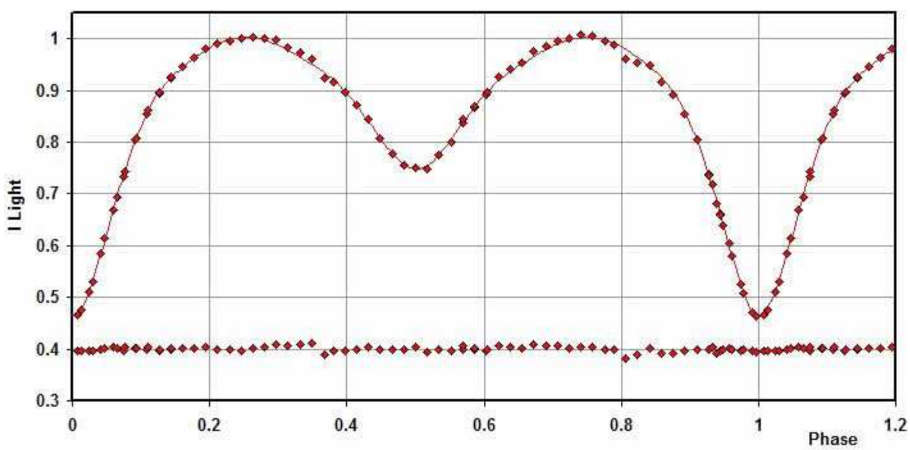

Figure 4. R_C light curves for V2197 Cyg – data, WD fit, and residuals.

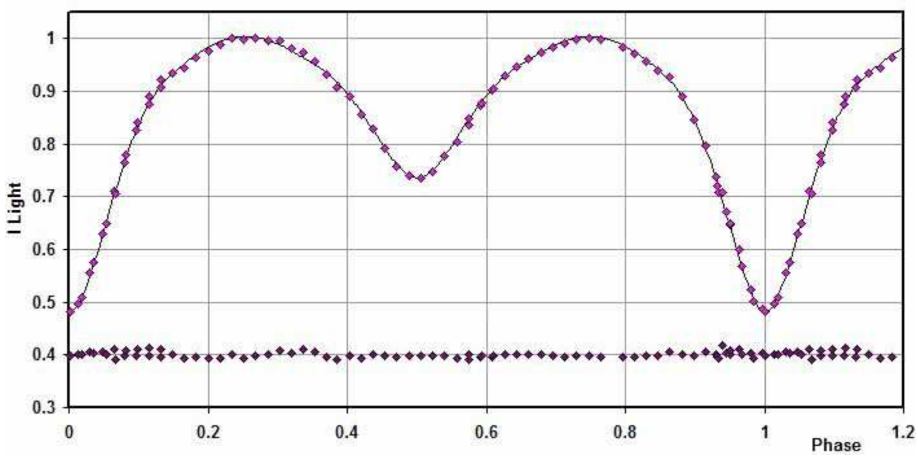

Figure 5. I_C light curves for V2197 Cyg – data, WD fit, and residuals.

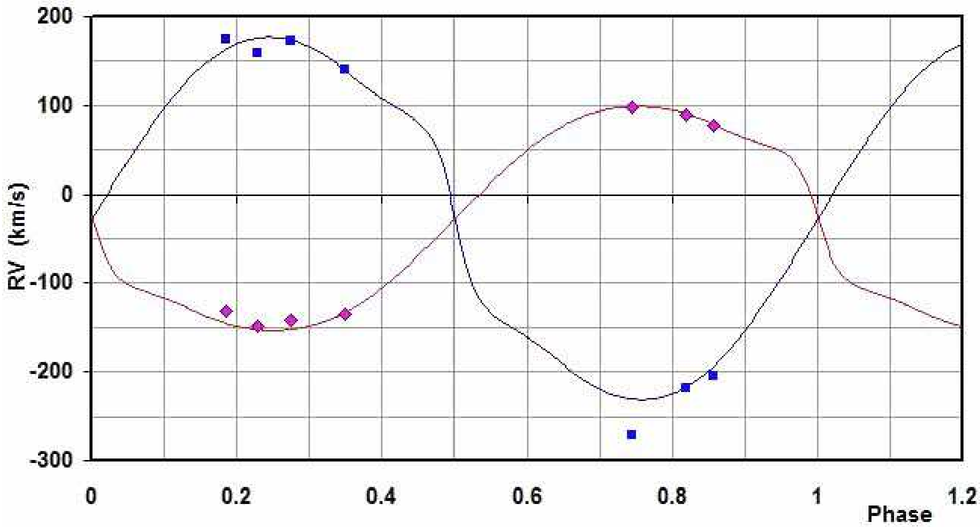

Figure 6. Radial velocity curves for V2197 Cyg – data and WD fit.

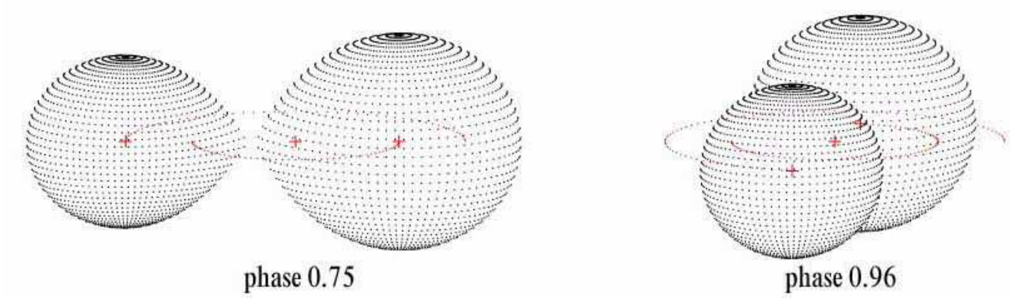

Figure 7. Binary Maker 7 representation of the system – at phases 0.75 and 0.97.

The WD output fundamental parameters and errors are listed in Table 5 using the data from the mode 5 solution (and are virtually identical with those from mode 6). From its temperature, star 2 was assumed to be spectral class K2. Most of the errors are output or derived estimates from the WD routines. From Kallrath & Milone (1999), the fill-out factor is $f = (\Omega_I - \Omega)/(\Omega_I - \Omega_O)$, where Ω is the modified Kopal potential of the system, Ω_I is that of the inner Lagrangian surface, and Ω_O, that of the outer Lagrangian surface, was also calculated.

To determine the distance r, the analysis proceeded as follows: first the WD routine gave the absolute bolometric magnitudes of each component; these were then converted to the absolute visual (V) magnitudes of both, $M_{V,1}$ and $M_{V,2}$, using the bolometric corrections BC = –0.120 and –0.420 for stars 1 and 2 respectively. The latter were taken from interpolated tables constructed from Cox (2000). The absolute V magnitude was then computed in the usual way, getting $M_V = 3.39 \pm 0.12$ magnitudes. The apparent magnitudes in the B and V passbands were $B = 12.10 \pm 0.01$ mag and $V = 11.65 \pm 0.01$ mag (presumed errors), taken from the Andronov et al. (1993). The colour excess (in B–V) was obtained in the usual way, by subtracting the tabular value of B–V (for that spectral class) from the observed value. This gave $E[B\text{–}V] = +0.07 \pm 0.08$ magnitudes.

Hence, for the mode 5 solution, a distance $r = 407$ pc was calculated from the standard

Table 5: Fundamental parameters.

Quantity	Observed	Tables	error	unit
Temperature, T_1	6820	6820	200	K
Temperature, T_2	5037	5026	200	K
Mass, m_1	1.25	1.48	0.02	$M_\odot$
Mass, m_2	0.75	0.74	0.01	$M_\odot$
Radius, R_1	1.36	1.38	0.02	$R_\odot$
Radius, R_2	1.07	0.80	0.02	$R_\odot$
$M_{bol,1}$	3.41	3.45	0.02	mag
$M_{bol,2}$	5.24	5.98	0.02	mag
$\log g_1$	4.27	4.33	0.01	cgs
$\log g_2$	4.25	4.51	0.03	cgs
Luminosity, L_1	3.57	4.54	0.07	$L_\odot$
Luminosity, L_2	0.66	0.36	0.01	$L_\odot$
Fill-out factor 1	–0.0003	—	—	—
Fill-out factor 2	0	—	—	—
Distance, r	407	—	50	pc

relation:

$$r = 10^{0.2(V-M_V-A_V+5)}\ \mathrm{pc} \tag{2}$$

The errors were assigned as follows: $\delta M_{bol,1} = \delta M_{bol,2} = 0.02$, $\delta BC_1 = 0.015$, $\delta BC_2 = 0.120$ (the variation over 1.5 spectral sub-classes), $\delta V = 0.02$, all in magnitudes. Combining the errors rigorously (i.e., by adding the variances) yielded an estimated error in r of 51 pc.

The distance estimate is in statistical agreement with the value of 320 ± 50 pc from the Gaia Catalogue[1] (Gaia Collaboration 2016, Lindegren et al. 2016).

For comparison, the tabular values for the fundamental parameters, taken from Cox (2000) for F3 and K2 main sequence stars, are given in Table 5. Of course, these apply to detached stars, which these are not; however, comparisons are useful. Star 1 is seen to be undermassive and underluminous for F3 (and the same for F4 which has a tabulated mass of 1.44 $M_\odot$ and a luminosity of 4.04 $L_\odot$) while star 2 has a larger radius (which is to be expected for one that fills its Roche lobe) and a higher luminosity (a function of its larger radius). The luminosities are fairly close but display differences, as one would expect for interacting stars.

In conclusion, the fundamental parameters of this system have been determined, albeit to a somewhat lower level of precision than one would like, mostly due to the uncertainty in the spectral class and the degree of interstellar absorption. Also, more accurate photometric data might enable one to distinguish definitively between the various modes.

Acknowledgements: It is a pleasure to thank the staff members at the DAO (especially Dmitry Monin, David Bohlender, and the late Les Saddlmyer) for their usual splendid help and assistance.

This work has made use of data from the European Space Agency (ESA) mission Gaia

[1] https://www.cosmos.esa.int/web/gaia/gaia-data

(https://www.cosmos.esa.int/gaia), processed by the Gaia Data Processing and Analysis Consortium (DPAC, https://www.cosmos.esa.int/web/gaia/dpac/consortium). Funding for the DPAC has been provided by national institutions, in particular the institutions participating in the Gaia Multilateral Agreement.

The eclipse timing (O–C) Excel file may be found online at Nelson (2016).

References:

Andronov, I. L., Chinarova, L. L., Kolesnikov, S. V., Shakhovskoy, N. M.. Shvechkova, N. A., 1993, *IBVS*, No. 3933

Andronov, I. L., Chikrigin, A. V., Kimeridze, G. N, 1994, *Odessa Astron. Pub.*, **7**, 89

Bradstreet, D.H., 1993, "Binary Maker 2.0 – An Interactive Graphical Tool for Preliminary Light Curve Analysis", in Milone, E.F. (ed.) Light Curve Modelling of Eclipsing Binary Stars, pp 151-166 (Springer, New York, N.Y.)

Cox, A. N., ed, 2000, Allen's Astrophysical Quantities, 4th ed., (Springer, New York, NY)

Csizmadia, S., Pasternacki, T., Dreyer, C., Cabrera, A., Erikson, A., Rauer, H., 2013, *A&A*, **549**, A9 DOI

Cutri, R.M., et al., 2003, VizieR On-line Data Catalog: II/246

Flower, P. J., 1996, *AJ*, **469**, 355 DOI

Gaia Collaboration, Prusti, T. et al. 2016, *A&A*, **595**, A1 DOI

Hoffman, D. I., Harrison, T. E., Coughlin, J. L., McNamara, B. J., Holtzman, J. A, Taylor G. E., and. Vestrand, W. T., 2008, *AJ*, **136**, 1067 DOI

Høg, E., et al., 2000, *A&A*, **355**, L27

Kallrath, J., Milone, E. F., 1999, Eclipsing Binary Stars–Modeling and Analysis (Springer-Verlag)

Kallrath, J., Milone, E.F., Terrell, D., and Young, A.T., 1998, *ApJ*, **508**, 308 DOI

Kreiner, J.M., 2004, *AcA*, **54**, 207

Kurucz, R.L., 2002, *Baltic Astron.*, **11**, 101

Lindegren, L. et al., 2016, *A&A*, **595**, A4 DOI

Margoni, R., Stagni, R., 1984, *A&AS*, **56**, 87

Nelson, R.H., 2009, Software, http://www.variablestarssouth.org/profilegrid_blogs/software-by-bob-nelson/

Nelson, R.H., 2010a, Spreadsheets, http://www.variablestarssouth.org/profilegrid_blogs/spreadsheets-by-bob-nelson/

Nelson, R.H., 2010b,"Spectroscopy for Eclipsing Binary Analysis" in The Alt-Az Initiative, Telescope Mirror & Instrument Developments (Collins Foundation Press, Santa Margarita, CA), R.M. Genet, J.M. Johnson and V. Wallen (eds)

Nelson, R.H., 2016, Bob Nelson's O–C Files, http://www.aavso.org/bob-nelsons-o-c-files

Nelson, R. H., Şenavcı, H.V. Baştürk, Ö., Bahar, E., 2014, *New Astron.*, **29**, 57 DOI

Rucinski, S. M., 2004, *IAUS*, **215**, 17

Skiff, B.A., 1997, *IBVS*, No. 4431

Terrell, D., 1994, Van Hamme Limb Darkening Tables, vers. 1.1.

Van Hamme, W., 1993, *AJ*, **106**, 2096 DOI

Wilson, R.E., Devinney, E.J., 1971, *ApJ*, **166**, 605 DOI

Wilson, R.E., 1990, *ApJ*, **356**, 613 DOI